Perturbation of *myo*-Inositol-1,4,5-Trisphosphate Levels during Agonist-Induced Ca^{2+} Oscillations

Jean-Yves Chatton, Yumei Cao, and Jörg W. Stucki
Institute of Pharmacology, University of Berne, CH-3010 Berne, Switzerland

ABSTRACT Agonist-induced Ca^{2+} oscillations in rat hepatocytes involve the production of *myo*-inositol-1,4,5-trisphosphate (IP_3), which stimulates the release of Ca^{2+} from intracellular stores. The oscillatory frequency is conditioned by the agonist concentration. This study investigated the role of IP_3 concentration in the modulation of oscillatory frequency by using microinjected photolabile IP_3 analogs. Photorelease of IP_3 during hormone-induced oscillations evoked a Ca^{2+} spike, after which oscillations resumed with a delay corresponding to the period set by the agonists. IP_3 photorelease had no influence on the frequency of oscillations. After photorelease of 1-(α-glycerophosphoryl)-D-*myo*-inositol-4,5-diphosphate ($GPIP_2$), a slowly metabolized IP_3 analog, the frequency of oscillations initially increased by 34% and declined to its original level within ~6 min. Both IP_3 and $GPIP_2$ effects can be explained by their rate of degradation: the half-life of IP_3, which is a few seconds, can account for the lack of influence of IP_3 photorelease on the frequency, whereas the slower metabolism of $GPIP_2$ allowed a transient acceleration of the oscillations. The phase shift introduced by IP_3 is likely the result of the brief elevation of Ca^{2+} during spiking that resets the IP_3 receptor to a state of maximum inactivation. A mathematical model of Ca^{2+} oscillations is in satisfactory agreement with the observed results.

INTRODUCTION

The phosphoinositide pathway producing *myo*-inositol-1,4,5-trisphosphate (IP_3) is involved in the release of Ca^{2+} ions from the intracellular stores in several nonexcitable cell types. In hepatocytes, hormones using this pathway include α-adrenergic hormones, vasopressin, angiotensin II, and adenosine nucleotides (ATP, ADP, AMP), among others, and the response evoked by these hormones is a periodical variation of cytosolic Ca^{2+} concentration called Ca^{2+} oscillations (Woods et al., 1986; Rooney et al., 1989), recently reviewed by Thomas et al. (1996). Above a certain concentration of agonist Ca^{2+} no longer oscillates, but remains chronically elevated.

The generation of Ca^{2+} oscillations has been intensely investigated at the theoretical level (Stucki and Somogyi, 1994; Sneyd et al., 1995). Based on the growing experimental data, the most recent mathematical models involve the participation of intracellular Ca^{2+} stores as a major source of Ca^{2+} for the oscillatory process. After binding of the agonist to its membrane receptor, the sequential activation of the phosphoinositide pathway components, i.e., G proteins, phospholipase C, and production of IP_3, results in the activation of the IP_3 receptor/Ca^{2+} channel located in the membrane of intracellular Ca^{2+} stores. Once activated, the IP_3 receptor/Ca^{2+} channel allows the rapid release of Ca^{2+} into the cytosol, which lasts until feedback mechanisms close the channel, allowing the cell to restore both cytosolic Ca^{2+} and intracellular store Ca^{2+} to their resting value. In the continuous presence of agonist, the Ca^{2+} spiking repeats itself in a periodical way at a stable frequency that is mainly determined by the agonist concentration.

Continuous G-protein activation (Osipchuk et al., 1990) or continuous IP_3 infusion (Petersen et al., 1991; Wakui et al., 1989) have been shown to be sufficient ingredients for induction of Ca^{2+} oscillations in pancreatic acinar cells in whole-cell patch-clamp experiments. A nonmetabolized analog of IP_3 was also shown to elicit Ca^{2+} oscillations in these cells (Wakui et al., 1989), which constitutes a strong argument against a possible role of pulsatile production or pulsatile metabolism of IP_3. In rat hepatocytes, however, the situation might not be identical, because Ca^{2+}-induced Ca^{2+} release, if present, does not represent a major mechanism of Ca^{2+} release, as in pancreatic acinar cells (Nathanson et al., 1992).

A higher agonist concentration is likely to result in a higher rate of IP_3 release in the cytosol and, consequently, a more pronounced stimulation of the IP_3 receptor. The present study investigates at the experimental level whether the frequency modulation imposed by the level of agonist is eventually controlled by the level of cytosolic IP_3 in rat hepatocytes. To this end, the effects of rapid release of IP_3 were investigated in nonstimulated hepatocytes and during agonist-induced trains of Ca^{2+} oscillations.

MATERIALS AND METHODS

Rat hepatocytes were isolated from male Wistar rats and attached to collagen-coated glass coverslips as described previously (Ubl et al., 1994).

Fluorescence microscopy

The fluorescence microscopy setup was composed of an image intensifier coupled to a video camera (Videoscope International, Washington, DC)

Received for publication 30 May 1997 and in final form 29 September 1997.

Address reprint requests to Dr. Jean-Yves Chatton, Institute of Pharmacology, University of Berne, Friedbühlstrasse 49, CH-3010 Berne, Switzerland. Tel.: +41-31-632-3281; Fax: +41-31-632-4992; E-mail: chatton@pki.unibe.ch.

0006-3495/98/01/523/09 $2.00

attached to an inverted microscope (Nikon, Tokyo, Japan). Cells were observed with a 100×/1.3 N.A. objective lens (Zeiss, Germany). A 100-W xenon lamp (Nikon) and a fluorescence filter wheel (Sutter Instruments, Novato, CA) were used to excite the specimen. The filter cube contained a 510-nm dichroic mirror and a 520-nm long-pass emission filter. The video image was digitized with an 8-bit image processor (Leutron, Glattburg, Switzerland), and a custom-made computer program allowed the selection of regions of interest and intensity measurement inside single cells. Fluorescence intensity measurements were made every 170–200 ms for kinetics measurements, or every 5–8 s during long-lasting trains of oscillations to minimize the illumination time.

Microinjection and flash photolysis

For cytosolic Ca^{2+} measurements the fluorescent probe Fluo-3 was chosen because its visible excitation at 480 nm does not cause unwanted photolysis of photolabile IP_3 analogs. Single isolated hepatocytes attached to coverslips were microinjected using pipettes beveled to ~50 MΩ (BV-10 Microelectrode Beveler, Sutter Instruments) and back-filled with an injection solution containing 2 mM Fluo-3 and 1.5 mM *myo*-inositol-1,4,5-trisphosphate $P^{4(5)}$-1-(2-nitrophenyl)ethyl ester (caged IP_3) or 1.4 mM 1-(α-glycerophosphoryl)D-*myo*-inositol-4,5-diphosphate $P^{4(5)}$-1-(2-nitrophenyl) ethyl ester(caged $GPIP_2$). Pressure injection was performed with the Eppendorf 5246 microinjection system (Eppendorf, Hamburg, Germany). The cells were then allowed to recover for 20–30 min before the experiments were started. The injected cells on coverslips were then transferred to the fluorescence microscope. Experiments were performed at room temperature.

The intensity of Fluo-3 signals at resting cytosolic Ca^{2+} levels for different intensities of illumination and image intensifier gain were compared to signals obtained for known Fluo-3 concentrations in whole-cell patch-clamp experiments (Chatton et al., 1995). Based on the calculated dilution of Fluo-3, the final caged IP_3 concentration in the injected cells was estimated to be 20–25 μM.

A high-intensity xenon flashlamp system (XF-10; Hi-Tech Scientific, Salisbury, England) was used to deliver flashes of UV light with a duration of 1 ms (Rapp and Güth, 1988). A UG-11 filter was inserted in the light path to select a band of UV light (300–390 nm), and a liquid light guide with quartz focusing lens was used to bring the light to the microscope stage and illuminate the cells with a 2–3-mm^2 spot.

The flash energy was adjusted by changing both the charge voltage and the combination of capacitors, to produce a maximum calculated output energy of 331 J. The timing of flash-lamp triggering and image acquisition was controlled by computer. A cytosolic Ca^{2+} response could be routinely observed after up to a dozen of consecutive flashes with caged IP_3, indicating that only a small fraction of the pool of caged compound injected underwent photolysis during one flash.

Solutions and materials

Bath solution was Ham's F12 culture medium containing 10 mM HEPES and 1.8 mM $CaCl_2$ and set to pH 7.4, or a similar solution containing (in mM) 145 NaCl, 5.6 KCl, 0.8 $MgSO_4$, 1.8 $CaCl_2$, 10 HEPES, 10 glucose. The pipette solution for microinjection contained (in mM) 138 K-glutamate, 8 NaCl, 5 $MgCl_2$, 1 EGTA, 0.5 $CaCl_2$, 10 HEPES and was adjusted to pH 7.2.

Caged IP_3 and (caged $GPIP_2$) were from Calbiochem (La Jolla, CA). Fluo-3 (K^+ salt) was from Molecular Probes (Eugene, OR). ADP, Ham's F12 medium, and bovine serum albumin were from Sigma (St. Louis, MO). The other chemicals were from Fluka (Buchs, Switzerland).

Expression of data

Data are presented as means ± SE. When appropriate, a nonpaired Student's *t*-test was performed to assess the statistical significance of differences.

Mathematical model of Ca^{2+} oscillations

In this study, we consider a minimal one-pool model that is an extended version of a previously published one (Somogyi and Stucki, 1991), in which the termination of a spike was caused by an emptying of the intracellular Ca^{2+} stores. Simultaneous measurements of Ca^{2+} in the cytosol and in the intracellular stores did not agree with this prediction (Chatton et al., 1995): the termination of a spike was not accompanied by an emptying of the stores, which pointed to an active participation of the IP_3 channel in the mechanism of spike termination. Therefore, we now consider the IP_3 channel to be in one of three states: closed, open, or inactivated (Fig. 1). The transition of the channel from the closed to the open state is brought about by increasing IP_3 and an autocatalytic effect of cytosolic Ca^{2+} on the opening probability of the channel. At higher concentrations of cytosolic Ca^{2+}, the channel tends to become inactivated. These assumptions are supported by the bell-shaped activation-inactivation characteristics of the channel by cytosolic Ca^{2+} (Bezprozvanny et al., 1991). It is most important to assume that the transition from the inactivated to the closed channel at low basal cytosolic Ca^{2+} is a slow process. There must be a refractory period in this transition that allows cytosolic Ca^{2+} to return to its basal level before the system becomes excitable again and exhibits oscillations of a limit-cycle type. Conversely, increasing the agonist stimulation would lead the system to an overstimulated state (i.e., chronically elevated cytosolic Ca^{2+}), the transition to which may show quasisinusoidal and damped oscillations (Somogyi and Stucki, 1991). In essence, the present model is a variant of the model formulated by Keizer's group (De Young and Keizer, 1992).

The second modification of the previous model consisted of explicitly introducing the formation and degradation of IP_3. At constant hormone concentration, IP_3 reaches a steady-state concentration sufficiently elevated

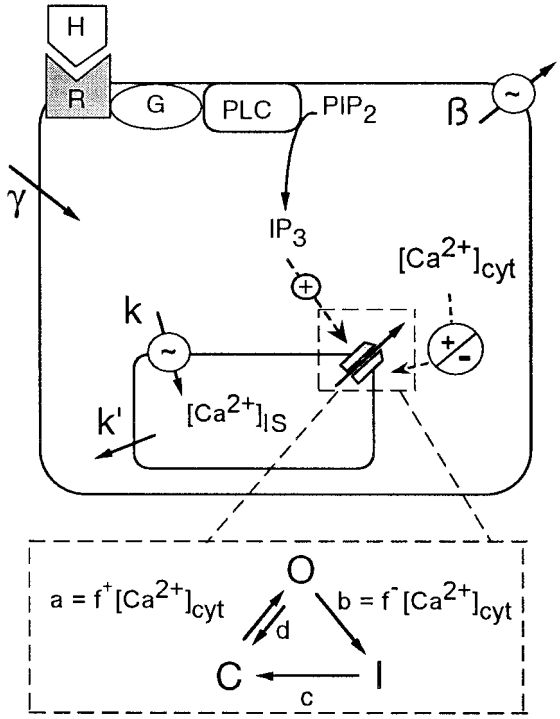

FIGURE 1 Model of Ca^{2+} oscillations in rat hepatocytes. The model is based on the three functional states of the IP_3 receptor/Ca^{2+} channel: open (O), closed (C), inactivated (I). Plain arrows indicate fluxes, dotted arrows indicate stimulatory or inhibitory action. H, hormone; R, receptor; G, G-proteins; PLC, phospholipase C; PIP_2, phosphatidyl-*myo*-inositol-4,5-bisphosphate; Ca^{2+}_{cyt}, cytosolic Ca^{2+}; Ca^{2+}_{IS}, intracellular store Ca^{2+}; γ, rate of Ca^{2+} entry; β, rate of active Ca^{2+} extrusion; *k*, rate of active Ca^{2+} pumping into the intracellular stores; *k*′, rate of Ca^{2+} leak from the stores.

to trigger oscillations or overstimulation. Application of a pulse of UV light to uncage IP_3 can be simulated by transiently perturbing the IP_3 level. The same goes for caged $GPIP_2$, which is assumed to react with the same receptor site on the IP_3 receptor/Ca^{2+} channel, but with an affinity and degradation rate different from that of IP_3.

The pertinent equations used in the model are shown in Table 1. A comprehensive analysis of the dynamic properties of this model as well as a linear stability analysis of its steady states have been performed as previously published (Stucki and Somogyi, 1994; Stucki, 1978) and will be presented in detail elsewhere.

All programs were coded in either Fortran (Absoft, Rochester Hills, MI) or Mathematica (Wolfram Research, Champaign, IL), and calculations were performed on a Macintosh 9500 computer.

RESULTS

Characterization of caged IP_3- and caged $GPIP_2$-induced Ca^{2+} response

In a first step, the response of isolated rat hepatocytes to rapid photorelease of IP_3 or its slowly metabolized analog $GPIP_2$ was characterized. Cells were individually microinjected with photolabile IP_3 analogs and Fluo-3 before the experiments. The amount of caged IP_3 or caged $GPIP_2$ injected (20–25 μM) was sufficient to obtain a Ca^{2+} response from multiple UV flashes.

Fig. 2 shows the typical time course of an IP_3-induced and $GPIP_2$-induced Ca^{2+} transient. To compare the two types of transients, the characteristic kinetic parameters were analyzed for each peak. The time delay (lag time) between the flash and the start of Ca^{2+} increase was measured. To estimate the rate of Ca^{2+} increase, the time from the end of the lag period to the half-maximum Ca^{2+} concentration ($t_{50\%}$) and to the peak maximum ($t_{100\%}$) were both measured. As can be seen in the graphs and in Table 2, both the lag time after photolysis of the two caged analogs and the rate of Ca^{2+} concentration increase are similar. In the case of IP_3-induced transients, the recovery of Ca^{2+} concentration followed single exponential kinetics with correlation coefficients greater than 0.990. As can be seen in Fig. 2, the kinetics of recovery was markedly different after a $GPIP_2$-induced spike. The recovery generally consisted of two phases: a first rapid phase followed by a slow phase, where Ca^{2+} gradually returned to baseline. The curves were fitted with a double exponential decay equation with mean correlation coefficients of 0.991. The kinetic parameters of the Ca^{2+} transients observed after photorelease of IP_3 and $GPIP_2$ are summarized in Table 2. All kinetic parameters of IP_3- and $GPIP_2$-induced transients were the same statistically, except the second phase of the $GPIP_2$ decay.

We next investigated the effects of flash intensity, i.e., of the amount of IP_3 delivered, on the Ca^{2+} response. A series

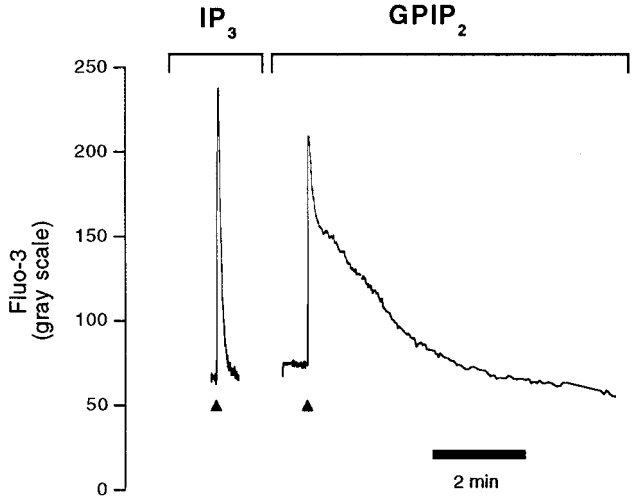

FIGURE 2 Kinetics of Ca^{2+} response after photolysis of caged IP_3 or caged $GPIP_2$. Isolated rat hepatocytes were microinjected with the Ca^{2+}-sensitive dye Fluo-3 and photolabile analogs of IP_3. Typical responses are presented for two different cells microinjected with caged IP_3 (*left*) or caged $GPIP_2$ (*right*), respectively. One-millisecond flashes of UV light were applied at times indicated by the closed triangles in the graph. Ca^{2+} signals were fluorimetrically measured using Fluo-3. Kinetic parameters and statistics of the two types of responses are summarized in Table 2.

TABLE 1 Equations used in the mathematical model of Ca^{2+} oscillations

$$\dot{Ca}^{2+}_{IS} = k \cdot Ca^{2+}_{cyt} - (k' + IP_3 \cdot O)(Ca^{2+}_{IS} - Ca^{2+}_{cyt})$$
$$\dot{Ca}^{2+}_{cyt} = \gamma - \beta \cdot Ca^{2+}_{cyt} + (k' + IP_3 \cdot O)(Ca^{2+}_{IS} - Ca^{2+}_{cyt})$$
$$\dot{O} = a \cdot (\sigma - I - O) - (b + d) \cdot O$$
$$\dot{I} = b \cdot O - c \cdot I$$
$$\dot{IP}_3 = k_p - k_d \cdot IP_3$$
$$a = a_0 \cdot (Ca^{2+}_{cyt})^n/(K_a^n + (Ca^{2+}_{cyt})^n)$$
$$b = b_0 \cdot (Ca^{2+}_{cyt})^m/(K_b^m + (Ca^{2+}_{cyt})^m)$$

Symbols: k, rate constant of Ca^{2+} pumping into intracellular stores; k', rate constant of Ca^{2+} leak from intracellular stores; O, C, I, open, closed, inactivated states of IP_3 receptor/Ca^{2+} channel; σ, sum of C, O, and I; a, rate function of C $\rightarrow$ O transition; b, rate function of O $\rightarrow$ I transition; c, rate constant of I $\rightarrow$ C transition; d, rate constant of O $\rightarrow$ C transition; a_0, intrinsic activity of activation; b_0, intrinsic activity of inactivation; γ, rate constant of Ca^{2+} entry; β, rate constant of Ca^{2+} extrusion; k_p, rate constant of IP_3 production; k_d, rate constant of IP_3 degradation; K_a, K_b, affinity constant of the IP_3 receptor to cytosolic Ca^{2+}. Exponents: n, m, Hill coefficients; indices: IS, intracellular stores; cyt, cytosol.

TABLE 2 Summary of kinetic parameters of Ca^{2+} spikes induced by photorelease of IP_3 or $GPIP_2$

	Caged IP_3	Caged $GPIP_2$
Lag time (s)	0.28 ± 0.04	0.20 ± 0.02
$t_{50\%}$ (s)	0.66 ± 0.12	0.59 ± 0.10
$t_{100\%}$ (s)	2.09 ± 0.37	1.83 ± 0.31
Recovery $t_{1/2}$ (s)	5.69 ± 0.99	(a) 4.06 ± 0.56
	—	(b) 98.11 ± 17.77*
n_{expt}, $n_{flashes}$	9, 37	5, 8

Kinetics parameters of Ca^{2+} transients obtained from n_{expt} separate experiments and $n_{flashes}$ are presented for caged IP_3- and caged $GPIP_2$-injected rat hepatocytes. The lag time is defined as the time elapsed between the 1-ms flash and the appearance of the Ca^{2+} response. The parameters $t_{50\%}$ and $t_{100\%}$ are defined as the time needed to reach 50% and 100%, respectively, of the maximum Ca^{2+} peak amplitude from the baseline. The half-time of recovery ($t_{1/2}$) for IP_3 was computed from single exponential kinetics fitted to the curve. $t_{1/2}$ for $GPIP_2$ was decomposed into a first rapid phase (a) and a second slower phase (b), obtained from fitting a double-exponential equation.

*Statistically different ($p < 0.0001$) from $t_{1/2}$ of IP_3 decay. No other kinetic parameters differed between caged IP_3 and caged $GPIP_2$ groups.

of five flashes of increasing energy in the range 50–220 J were applied to single cells from four experiments. The kinetics parameters of Ca^{2+} transients revealed that the lag time, $t_{50\%}$ and $t_{100\%}$, decreased with increasing flash intensity (data not shown). Increasing the energy of flash also increased the amplitude of spiking. Fig. 3 *A* shows the spike amplitude plotted against the energy of flash. Because of the variation in the amount of Ca^{2+} dye Fluo-3 injected, the ordinate has been normalized to 100% at 151 J. The graph shows that, in the range of energy considered, a quasilinear relationship exists between the amplitude of Ca^{2+} spiking and the energy delivered during a flash. It should be noted that below a certain threshold of energy, ~40 J, no Ca^{2+} transient was evoked, and there was a tendency toward plateauing at higher energy values (data not shown), which is consistent with either a saturation of IP_3 receptors or a maximum Ca^{2+} release from the intracellular stores. It should also be noted that each flash depletes the pool of available caged IP_3 by an amount proportional to the flash intensity, which could cause the steepness of the amplitude-energy relationship to be underestimated somewhat.

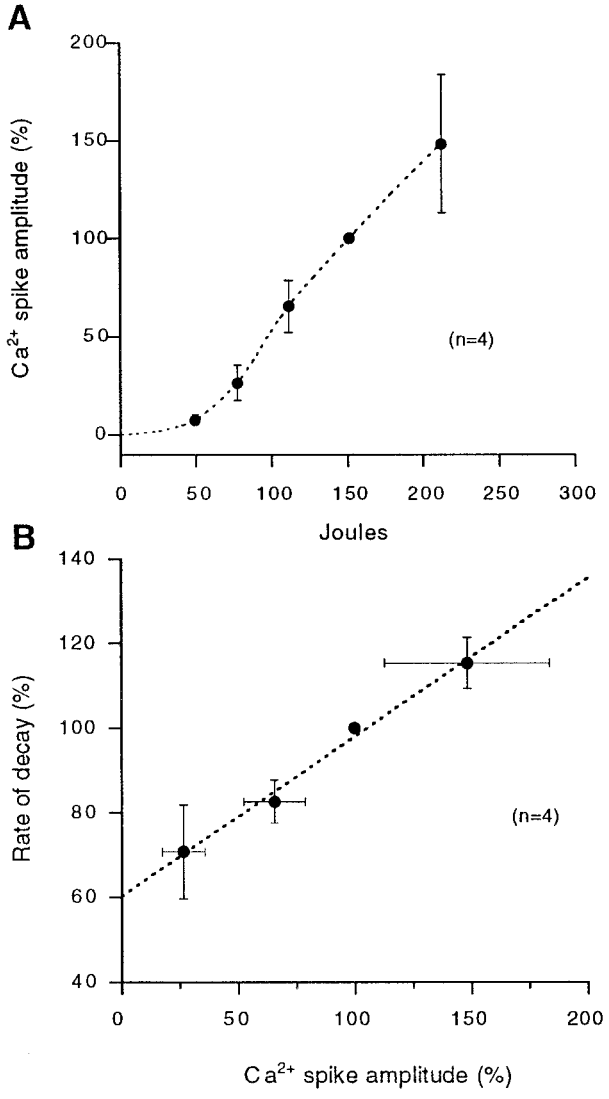

FIGURE 3 Relationship between Ca^{2+} spike amplitude and flash energy. (*A*) The energy of electrical discharge during flashes (Joules) was varied while measuring IP_3-induced Ca^{2+} transients using Fluo-3. Because of the variability in the amount of fluorescent dye present in the cells, the amplitude of Ca^{2+} transients was normalized to 100% at 151 J. (*B*) The rate of decay (s^{-1}) normalized to the rate measured at 151 J is plotted against the Ca^{2+} spike amplitude. The decay data were obtained from the experiments described in *A*. Data are means ± SE from four separate preparations.

These experiments showed that, as was observed with guinea pig hepatocytes (Chiavaroli et al., 1994), in rat hepatocytes, the amplitude of Ca^{2+} spikes is dependent on the amount of IP_3 delivered, whereas increasing the dose of an IP_3-producing agonist like phenylephrine does not influence the amplitude of spiking, but only the frequency of oscillations.

In this series of experiments, the recovery phase of Ca^{2+} spikes was found to occur faster with increasing flash energy. As a direct consequence (Fig. 3 *B*), the rate of Ca^{2+} recovery was found to be proportional to the amplitude of the Ca^{2+} spikes. This observation is consistent with negative feedback imposed by Ca^{2+} on its own release from the stores by the IP_3 receptor (Bezprozvanny et al., 1991).

Photorelease of IP_3 and $GPIP_2$ during agonist-induced Ca^{2+} oscillations

As discussed above, increasing the dose of several hormones administered to oscillating cells leads to a frequency increase in Ca^{2+} oscillations. An increase in agonist concentration should induce a stronger activation of G proteins and phospholipase C, and ultimately result in a higher production of intracellular IP_3. The next series of experiments was designed to investigate the effects of a rapid perturbation of the IP_3 concentration during sustained hormone-induced Ca^{2+} oscillations.

Single hepatocytes microinjected with Fluo-3 and caged IP_3 were stimulated with the α-adrenergic agonist phenylephrine at a concentration adequate to obtain cytosolic Ca^{2+} oscillations (Fig. 4 *A*). After a few regularly spaced oscillatory transients, a flash of UV light was applied while the Ca^{2+} concentration was at its resting level, i.e., during the interval between transients. As can be seen in the figure, the photorelease of IP_3 (*arrowheads*) evoked a fast Ca^{2+} spike, and when Ca^{2+} had recovered, normal oscillatory spiking resumed. Fig. 4 *B* depicts the frequency variations (min^{-1}) of Ca^{2+} oscillations, calculated from the time intervals between Ca^{2+} maxima, along the experiment. The open symbols and arrows indicate the IP_3-triggered spikes. In the example shown, the second flash was triggered as soon as Ca^{2+} had reached the baseline after the oscillatory peak, whereas the first flash occurred somewhat later in the interval. In both cases, however, the Ca^{2+} peak that followed the IP_3-induced spike and the subsequent ones came after the same time interval as was found before the flashes. Thus, photorelease of IP_3 induced a Ca^{2+} spike and reset the phase of oscillations without altering the frequency.

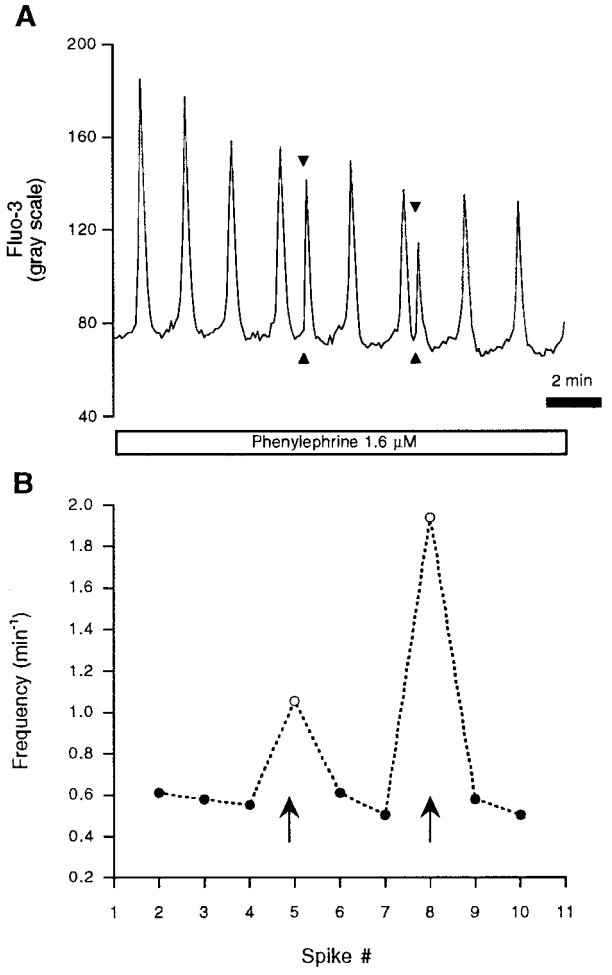

FIGURE 4 Photorelease of IP_3 during phenylephrine-induced cytosolic Ca^{2+} oscillations. (*A*) Hepatocytes injected with caged IP_3 were stimulated with phenylephrine to elicit sustained Ca^{2+} oscillations, measured with Fluo-3. At times indicated by the set of closed triangles, flashes of UV light were applied and the released IP_3 immediately induced Ca^{2+} mobilization. The following oscillatory spike came with a delay that corresponded to the period set by the agonist. (*B*) The frequency of oscillation (min^{-1}) calculated from the period between Ca^{2+} spikes in the experiment shown in *A* is plotted for each measured Ca^{2+} transient. Closed circles are agonist-induced oscillatory transients. Open circles and arrows indicate caged IP_3-induced Ca^{2+} spikes. The oscillatory Ca^{2+} transient that followed the flash-induced spike arrived with the same frequency as the initial frequency. A representative experiment from a total of four is shown.

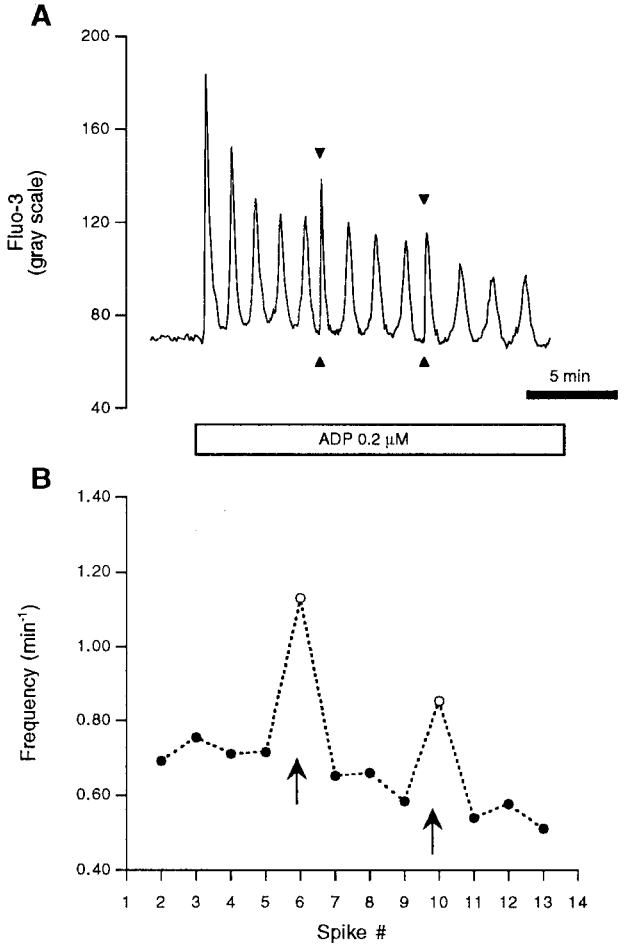

FIGURE 5 Photorelease of IP_3 during ADP-induced Ca^{2+} oscillations. Experiments were performed using the same protocol as in Fig. 4, but with ADP as the agonist. The figure shows typical traces from four experiments.

To examine whether this feature was specific to α-adrenergic hormones, two other agonists able to elicit Ca^{2+} oscillations but acting on different classes of receptors were tested, namely adenosine diphosphate (ADP), an agonist of the P_{2y} purinoceptor (Dixon et al., 1990), and (Arg^8) vasopressin (vasopressin), which activates V_1 receptors in hepatocytes (Dasso and Taylor, 1994). As can be seen in Figs. 5 and 6, the same phenomenon was observed when the agonist was ADP ($n = 4$ experiments) or vasopressin ($n = 4$ experiments). These experiments indicated that the observed phase shift of oscillations produced by IP_3 photorelease and its lack of effect on the frequency of Ca^{2+} oscillations were not restricted to Ca^{2+} oscillations induced by α-adrenergic stimulation, but appeared to apply to all agonists that use the phosphoinositide signaling pathway in hepatocytes.

We then asked whether the extent of phase shift introduced by IP_3 photorelease depended on when it was applied in the interval between oscillatory transients. Fig. 7 shows that IP_3 photorelease triggered at different time points after an oscillatory transient produced a shift of ~100% of the basal frequency, regardless of whether it occurred just after an oscillatory transient or near the end of the normal period imposed by the agonist concentration.

The fact that photorelease of IP_3 did not produce any increase in the frequency of Ca^{2+} oscillations led us to consider the possibility that the degradation of the IP_3 molecules photoreleased was occurring rapidly enough to prevent any frequency effect. If this were really the case, one would expect to obtain different results by using non-metabolized analogs of IP_3.

The same protocol as in Figs. 4–6 was therefore applied with hepatocytes microinjected with caged $GPIP_2$. Stimulation with phenylephrine evoked sustained Ca^{2+} oscillations, and when a flash of UV light was triggered in the same

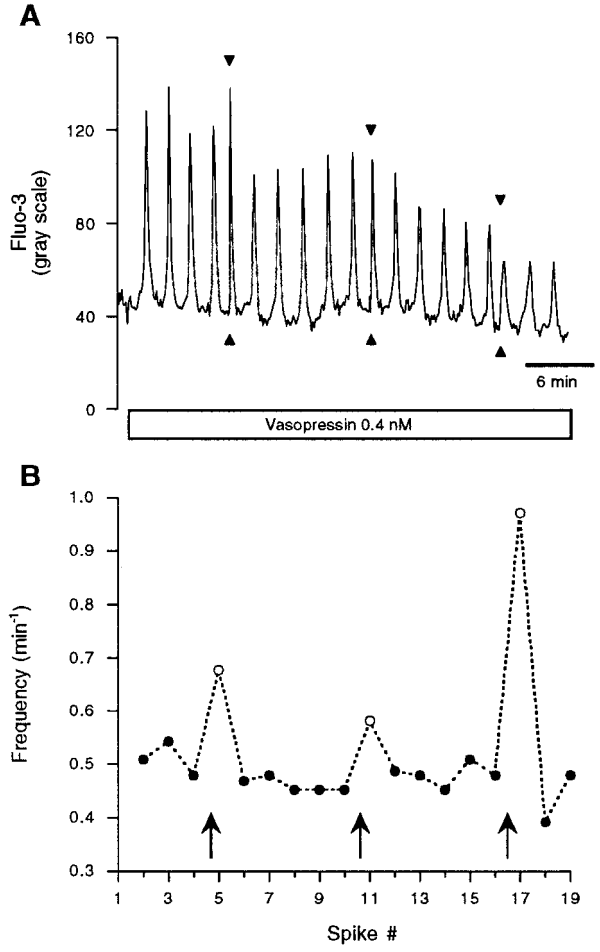

FIGURE 6 Photorelease of IP_3 during vasopressin-induced Ca^{2+} oscillations. Experiments were performed using the same protocol as in Fig. 4, but with vasopressin as the agonist. The figure is a representative experiment of four.

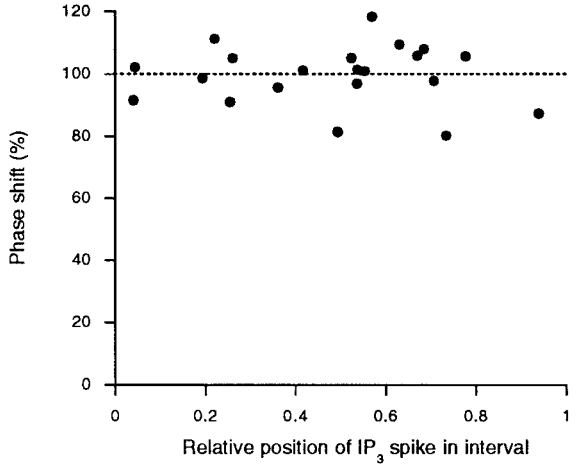

FIGURE 7 Relationship between the extent of phase shift and the position of IP_3 photorelease in the interval of Ca^{2+} oscillations. The amount of phase shift in percentage of the oscillatory frequency imposed by the hormone is plotted against the position of IP_3 photorelease within the interval. The position of IP_3-induced spike relative to the preceding oscillatory Ca^{2+} transient was scaled to the basal interval imposed by the agonist. Data are pooled from experiments using the agonists phenylephrine, ADP, or vasopressin.

range of energy as for caged IP_3 experiments, an immediate overstimulated Ca^{2+} response was observed in five experiments (data not shown). Such a response is typically found when the agonist concentration exceeds a certain threshold, where Ca^{2+} oscillations turn into a chronic elevation of cytosolic Ca^{2+} (also called overstimulation). The flash intensity was therefore reduced and the same protocol repeated. Fig. 8 *A* shows that a response considerably different from that of the caged IP_3 experiments was obtained. First, the oscillatory Ca^{2+} transient that directly followed the $GPIP_2$-induced spike came with a shorter delay than the regular oscillatory period. Second, the frequency of the oscillatory peaks that followed $GPIP_2$ photorelease was higher compared with the basal frequency and gradually decreased to the original value imposed by the agonist concentration (Fig. 8 *B*).

To quantify these effects, the mean frequency of Ca^{2+} oscillations induced by phenylephrine was calculated from the oscillatory period before photolysis of the caged compounds and compared with the period between the IP_3- or $GPIP_2$-induced Ca^{2+} spike and the next oscillatory transient. Whereas the photorelease of IP_3 did not produce any increase in frequency (103.3 ± 2.7%, $n = 5$ experiments, 9 flashes), $GPIP_2$ significantly increased the frequency to 134.3 ± 6.3% ($n = 7$ experiments, 15 flashes, $p = 0.001$).

We postulate that the phase shift produced by IP_3, its lack of effect on the frequency of oscillations, and the effects of $GPIP_2$ can be decomposed into two phenomena: 1) the transient elevation of Ca^{2+} induced by the IP_3 delivery puts the IP_3 receptor in an inactivated state (i.e., resets the phase of oscillations), and 2) the degradation of IP_3 occurs at the same rate as or faster than the recovery of Ca^{2+} to the baseline, meaning that the level of IP_3 has decayed to the level imposed by the agonist, while the IP_3 receptor was still in an inactivated state.

To test whether these hypotheses are sound, we used the mathematical model of Ca^{2+} oscillations described above and simulated the photorelease of IP_3 and $GPIP_2$, taking into account their rates of degradation. Fig. 9 shows the results of such simulations, where the rate of degradation of $GPIP_2$ was set to a 17-fold slower value than IP_3. Cytosolic Ca^{2+} oscillations started as soon as IP_3 was increased to its elevated steady state. Cytosolic oscillations were accompanied by periodic depletion of the intracellular store. Toward the end of the presented simulation, the Ca^{2+} pumping into the stores was stopped, which emptied the stores. As can be seen in the graph, the stores were only partially depleted during oscillations, as was observed experimentally (Chatton et al., 1995), indicating that spike termination is not caused by the emptying of the stores. These simulations yielded results strikingly similar to those of their experimental counterpart: the simulated IP_3 release inserted a phase shift without accelerating the oscillations, whereas a

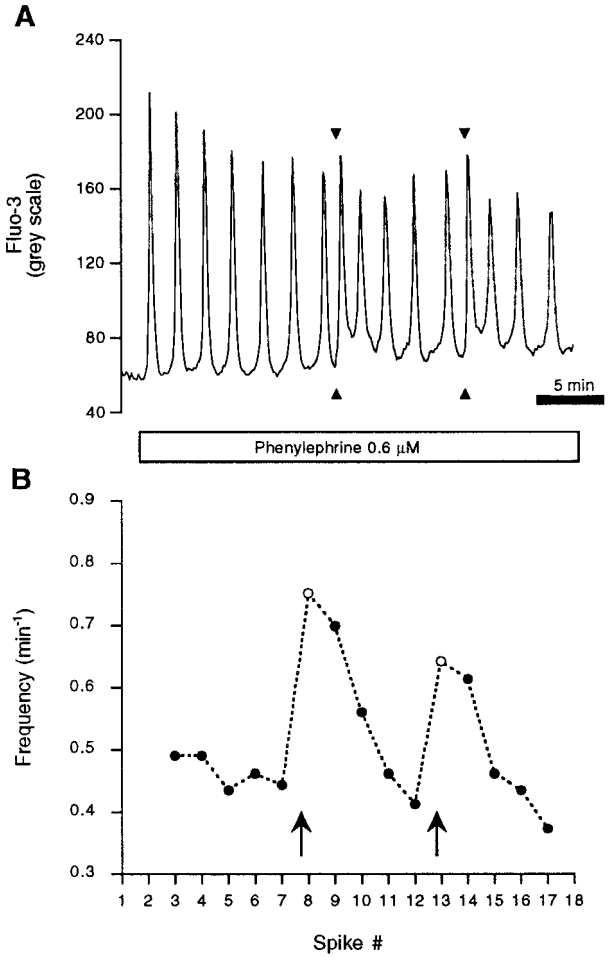

FIGURE 8 Photorelease of $GPIP_2$ during phenylephrine-induced cytosolic Ca^{2+} oscillations. (*A*) Hepatocytes injected with caged $GPIP_2$ were stimulated with phenylephrine to elicit sustained Ca^{2+} oscillations, measured with Fluo-3. At times indicated by the set of closed triangles, flashes were applied and the released $GPIP_2$ promptly induced Ca^{2+} mobilization. The following oscillatory spikes came with a shorter delay than the one set by the agonist. The figure depicts a representative experiment from a total of seven. (*B*) The frequency of oscillation (min^{-1}) calculated from the period between Ca^{2+} spikes in the experiment presented in *A* is plotted for each measured Ca^{2+} transient. Closed circles represent agonist-induced oscillatory transients and open circles and arrows indicate caged $GPIP_2$-induced spikes. The oscillatory Ca^{2+} transients that follow the $GPIP_2$-induced spikes have an increased frequency that progressively declined back to the initial frequency.

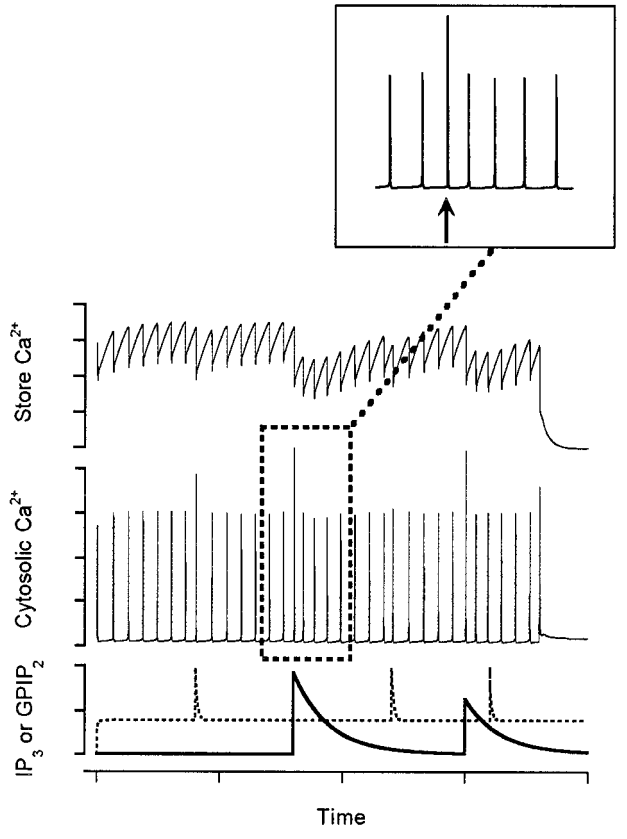

FIGURE 9 Computer simulations of IP_3 and $GPIP_2$ photorelease during agonist-induced Ca^{2+} oscillations. Variations of intracellular store Ca^{2+} and cytosolic Ca^{2+} are shown in the upper and middle panels, respectively. The lower panel represents the time course of IP_3 (*dotted trace*) and $GPIP_2$ (*bold trace*) changes. Toward the end of the simulated experiment, inhibition of the intracellular store Ca^{2+} pump was simulated, causing an emptying of the stores, a concomitant Ca^{2+} release into the cytosol, and the immediate cessation of the oscillations. All data are in arbitrary units. The following parameters were used in the simulations: $k' = 0.01$, $k = 3.0$, $k_p = 0.45$, $k_d = 0.12$, $\beta = 1.0$, $\gamma = 3.0$, $a_0 = 2.0$, $K_a = 15.0$, $n = 3$, $b_0 = 5.0$, $K_b = 0.2$, $m = 2$, $c = 0.001$, $d = 0.01$, $\sigma = 50$ (see Fig. 1 and Table 1 for details on the model).

simulated $GPIP_2$ release resulted in a transient frequency increase in the oscillations.

DISCUSSION

The purpose of this study was to investigate the role of IP_3 in setting the frequency of agonist-induced cytosolic Ca^{2+} oscillations in rat hepatocytes. This study has directly demonstrated, by using transient as well as more prolonged perturbation of IP_3 receptor stimulation, that the level of IP_3 indeed influences agonist-induced Ca^{2+} oscillations.

Kinetic properties of IP_3 and $GPIP_2$-induced Ca^{2+} mobilization

Photolysis of caged IP_3 produced Ca^{2+} spikes that had both faster activation kinetics and a faster return to baseline than agonist-induced Ca^{2+} oscillatory transients. This different behavior can be explained by the photochemical reaction that releases IP_3 with a half-time of 3 ms or less (Walker et al., 1987), which is orders of magnitude more rapid than the phospholipase C-mediated production of IP_3 (Chiavaroli et al., 1994) in hepatocytes. In addition, in a bolus release of IP_3, as opposed to a continuous IP_3 production by the phospholipase C, one can expect that IP_3 will disappear quickly. Metabolism of IP_3 has been shown to occur with a half-time of a few seconds (Hughes et al., 1988; Wang et al., 1995; Bird et al., 1992). The half-life of Ca^{2+} recovery measured in the present study (5.7 sec) is very close to the half-life of IP_3 metabolism of 7.6 s measured in rat parotid

acinar cells (Hughes et al., 1988) and of 9 s obtained in neuroblastoma cells (Wang et al., 1995). Therefore, the recovery could be explained, in principle, solely by the degradation of the photoreleased IP_3.

A strikingly different Ca^{2+} response was observed after rapid photorelease of $GPIP_2$. $GPIP_2$ appears to possess an affinity for the IP_3 receptor about one order of magnitude lower than that of IP_3, but to be capable nevertheless of maximally activating Ca^{2+} signaling (Bird et al., 1992). In our experiments, photorelease of $GPIP_2$ resulted in Ca^{2+} signals with activation kinetics indistinguishable from that of IP_3, but with recovery kinetics consisting of more than one phase. The first phase of recovery had a half-time similar to that of the IP_3 recovery. A second phase occurred with ~25-fold slower kinetics. Very similar kinetics values were observed with guinea pig hepatocytes (Wootton et al., 1995) when another nonmetabolized IP_3 analog, 5-thio-IP_3, was used. A complex Ca^{2+} sensitivity of the IP_3 receptor has been demonstrated with isolated receptors (Bezprozvanny et al., 1991) and various intact cell preparations (Oancea and Meyer, 1996): an increasing Ca^{2+} concentration activated the IP_3 receptor up to a critical concentration, where Ca^{2+} turns into an inhibitory factor. We hypothesize that the initial phase of recovery from photorelease of $GPIP_2$ originated from a rapid but partial inactivation of the IP_3 receptor caused by the elevated Ca^{2+}. The second phase would be due primarily to the slow metabolism of $GPIP_2$, which occurs over several minutes (Bird et al., 1992).

Because the first phase of $GPIP_2$ recovery occurred at the same rate as the recovery in an IP_3-induced Ca^{2+} transient, we propose that the Ca^{2+}-induced inactivation of the IP_3 receptor and the metabolism of IP_3 have the same or very close kinetics and could not be distinguished in our measurements.

Perturbation of cytosolic IP_3 concentration during agonist-induced Ca^{2+} oscillations

It has been shown in many investigations involving hepatocytes as well as other types of cells that stimulation with certain agonists leads to cytosolic free Ca^{2+} oscillations, the frequency of which is determined by the concentration of the applied agonist (Thomas et al., 1996). This frequency modulation rather than amplitude modulation of signaling is thought to play a role in certain cellular processes. Increasing the dose of agonist, which results in frequency increase, should be accompanied by a stronger activation of G proteins, phospholipase C, and ultimately a higher level of cytosolic IP_3. Most of the recent models describing Ca^{2+} oscillations would predict that the parameter eventually responsible for setting the pace of oscillations is the level of IP_3 (Stucki and Somogyi, 1994), determined by the counteracting processes of generation and degradation of IP_3.

To investigate this issue experimentally, we took advantage again of the technique of flash photolysis, with microinjected photolabile precursors of IP_3 to perturb the cytosolic level of IP_3 during sustained Ca^{2+} oscillations. Photolysis of caged IP_3 triggered during the interval between oscillatory transients resulted in the generation of a rapid Ca^{2+} spike. This observation indicated that, in rat hepatocytes, if a refractory state exists between two oscillatory transients, it has to be considered partial and reversible. Unexpectedly, photorelease of IP_3 during Ca^{2+} oscillations had no influence on the frequency of oscillations, but had the effect of introducing a phase shift in the oscillations or, in other words, of resetting the clock. The influence of IP_3 photorelease on the oscillatory pattern can be due to a direct action of IP_3 on its intracellular receptor as well as to an indirect one through elevated cytosolic Ca^{2+} that followed the IP_3 release. We observed that rapid photorelease of IP_3 consistently introduced a shift of the same duration as the period set by the agonist concentration, regardless of when it was applied in the interval between two oscillatory transients (i.e., just after a transient, in the middle or near the end of the period). One can therefore conclude that its effect is to reset the IP_3 receptor to its state of maximum inactivation.

The fact that photorelease of IP_3 did not increase the frequency of Ca^{2+} oscillations speaks again in favor of a highly active metabolism of IP_3 (Hughes et al., 1988; Wang et al., 1995) that is capable of restoring the level of IP_3 to its "preflash" level, probably at the same time as or before Ca^{2+} has returned to baseline. The implication is that the parameter that resets the phase of oscillations is probably the cytosolic Ca^{2+} concentration itself. As seen in Fig. 3 *B* as well as in isolated IP_3 receptors (Bezprozvanny et al., 1991), an elevated cytosolic Ca^{2+} has the tendency to inactivate the release of Ca^{2+} from the stores. Another indication that this effect also occurs in rat hepatocytes came from recent experiments (Chatton et al., 1997), during which photorelease of IP_3 during maximum α-agonist stimulation—where cytosolic Ca^{2+} remains chronically elevated—induced a Ca^{2+} spike above the elevated baseline. This spike was followed by an undershooting of the Ca^{2+} signal and brief oscillations around the elevated steady state. We believe that the observed undershooting is consistent with the Ca^{2+} spike causing a transient inactivation of the IP_3 receptor.

If the lack of effect of caged IP_3 on the oscillatory frequency was due to its fast metabolism, then releasing a nonmetabolized analog of IP_3 should affect the frequency of oscillations. Caged $GPIP_2$ was chosen for this purpose, even though it undergoes a slow degradation, ~200-fold slower that IP_3 in mouse lacrimal acinar cells (Bird et al., 1992), but probably somewhat faster in rat hepatocytes. For computer simulations, we used a $GPIP_2$ degradation rate 17-fold slower than that of IP_3, based on the kinetics of recovery presented in Table 2.

Photorelease of $GPIP_2$, indeed, resulted in a very different type of response during agonist-induced Ca^{2+} oscillations. First, an overstimulatory response was readily induced when the energy of photolysis was a little too high, which has never been observed with caged IP_3. Second,

when overstimulation was avoided by reducing the amount of light delivered, an increase in frequency of the Ca^{2+} transients after the photorelease was observed. This acceleration was transient, however, and lasted up to ~6 min, consistent with the expected rate of $GPIP_2$ metabolism. Computer simulations based on a minimal model that takes into account the respective degradation rates of IP_3 and $GPIP_2$ effectively reproduced the observed cell responses to photorelease of IP_3 analogs.

Taken together, our experiments, supported by mathematical modeling, demonstrated that an enhanced activation of IP_3 receptors increases the frequency of oscillations and indicated that a refractory state is initiated by a Ca^{2+} spike. The duration of this state depends on the amount of IP_3 present. Thus the level of IP_3 directly influences the frequency of oscillations, the elevated Ca^{2+} being responsible mainly for putting the system into a state of reversible inactivation.

The authors gratefully acknowledge Prof. E. Niggli (Institute of Physiology, University of Berne) for his valuable help with the flash photolysis technique.

This study was supported by grants 31-39605.93 and 31-49745.96 from the Swiss National Science Foundation.

REFERENCES

Bezprozvanny, I., J. Watras, and B. E. Ehrlich. 1991. Bell-shaped calcium-response curves of $Ins(1,4,5)P_3$- and calcium-gated channels from endoplasmic reticulum of cerebellum. *Nature.* 351:751–754.

Bird, G. St. J., J. F. Obie, and J. W. Putney, Jr. 1992. Sustained Ca^{2+} signaling in mouse lacrimal acinar cells due to photolysis of "caged" glycerophosphoryl-myo-inositol 4,5-bisphosphate. *J. Biol. Chem.* 267: 17722–17725.

Chatton, J.-Y., Y. Cao, and J. W. Stucki. 1997. Agonist-specific behavior of the intracellular calcium response in rat hepatocytes. *Biochem. J.* (in press).

Chatton, J.-Y., H. Liu, and J. W. Stucki. 1995. Simultaneous measurements of Ca^{2+} in the intracellular stores and the cytosol of hepatocytes during hormone-induced Ca^{2+} oscillations. *FEBS Lett.* 368:165–168.

Chiavaroli, C., G. St. J. Bird, and J. W. Putney, Jr. 1994. Delayed "all-or-none" activation of inositol 1,4,5-triphosphate-dependent calcium signaling in single rat hepatocytes. *J. Biol. Chem.* 269: 25570–25575.

Dasso, L. L. T., and C. W. Taylor. 1994. Interaction between Ca^{2+}-mobilizing receptors and their G proteins in hepatocytes. *J. Biol. Chem.* 269:8647–8652.

De Young, G. W., and J. Keizer. 1992. A single-pool inositol 1,4,5-trisphosphate-receptor-based model for agonist-stimulated oscillations in Ca^{2+} concentration. *Proc. Natl. Acad. Sci. USA.* 89:9895–9899.

Dixon, C. J., N. M. Woods, K. S. R. Cuthbertson, and P. H. Cobbold. 1990. Evidence for two Ca^{2+}-mobilizing purinoceptors on rat hepatocytes. *Biochem. J.* 269:499–502.

Hughes, A. R., H. Takemura, and J. W. Putney, Jr. 1988. Kinetics of inositol 1,4,5-trisphosphate and inositol cyclic 1:2,4,5-trisphosphate metabolism in intact rat parotid acinar cells. Relationship to calcium signalling. *J. Biol. Chem.* 263:10314–10319.

Nathanson, M. H., P. J. Padfield, A. J. O'Sullivan, A. D. Burgstahler, and J. D. Jamieson. 1992. Mechanism of Ca^{2+} wave propagation in pancreatic acinar cells. *J. Biol. Chem.* 267:18118–18121.

Oancea, E., and T. Meyer. 1996. Reversible desensitization of inositol trisphosphate-induced calcium release provides a mechanism for repetitive calcium spikes. *J. Biol. Chem.* 271:17253–17260.

Osipchuk, Y. V., M. Wakui, D. I. Yule, D. V. Gallacher, and O. H. Petersen. 1990. Cytoplasmic Ca^{2+} oscillations evoked by receptor stimulation, G-protein activation, internal application of inositol trisphosphate or Ca^{2+}: simultaneous microfluorimetry and Ca^{2+} dependent Cl^- current recording in single pancreatic acinar cells. *EMBO J.* 9:694–704.

Petersen, C. C. H., E. C. Toescu, B. V. L. Potter, and O. H. Petersen. 1991. Inositol triphosphate produces different patterns of cytoplasmic Ca^{2+} spiking depending on its concentration. *FEBS Lett.* 293:179–182.

Rapp, G., and K. Güth. 1988. A low cost high intensity flash device for photolysis experiments. *Pflügers Arch.* 411:200–203.

Rooney, T. A., E. J. Sass, and A. P. Thomas. 1989. Characterization of cytosolic calcium oscillations induced by phenylephrine and vasopressin in single fura-2-loaded hepatocytes. *J. Biol. Chem.* 264:17131–17141.

Sneyd, J., J. Keizer, and M. J. Sanderson. 1995. Mechanisms of calcium oscillations and waves: a quantitative analysis. *FASEB J.* 9:1463–1472.

Somogyi, R., and J. W. Stucki. 1991. Hormone-induced calcium oscillations in liver cells can be explained by a simple one pool model. *J. Biol. Chem.* 266:11068–11077.

Stucki, J. W. 1978. Stability analysis of biochemical systems—a practical guide. *Prog. Biophys. Mol. Biol.* 33:99–187.

Stucki, J. W., and R. Somogyi. 1994. A dialogue on Ca^{2+} oscillations: an attempt to understand the essentials of mechanisms leading to hormone-induced intracellular Ca^{2+} oscillations in various kinds of cell on a theoretical level. *Biochim. Biophys. Acta.* 1183:453–472.

Thomas, A. P., G. St. J. Bird, G. Hajnoczky, L. D. Robb-Gaspers, and J. W. Putney, Jr. 1996. Spatial and temporal aspects of cellular calcium signaling. *FASEB J.* 10:1505–1517.

Ubl, J. J., S. Chen, and J. W. Stucki. 1994. Anti-diabetic biguanides inhibit hormone-induced intracellular Ca^{2+} concentration oscillations in rat hepatocytes. *Biochem. J.* 304:561–567.

Wakui, M., B. V. L. Potter, and O. H. Petersen. 1989. Pulsatile intracellular calcium release does not depend on fluctuations in inositol trisphosphate concentration. *Nature.* 339:317–320.

Walker, J. W., A. V. Somlyo, Y. E. Goldman, A. P. Somlyo, and D. R. Trentham. 1987. Kinetics of smooth and skeletal muscle activation by laser pulse photolysis of caged inositol 1,4,5-trisphosphate. *Nature.* 327:249–252.

Wang, S. S. H., A. A. Alousi, and S. H. Thompson. 1995. The lifetime of inositol 1,4,5-trisphosphate in single cells. *J. Gen. Physiol.* 105: 149–171.

Woods, N. M., K. S. R. Cuthbertson, and P. H. Cobbold. 1986. Repetitive transient rises in cytoplasmic free calcium in hormone-stimulated hepatocytes. *Nature.* 319:600–602.

Wootton, J. F., J. E. T. Corrie, T. Capiod, J. Feeney, D. R. Trentham, and D. C. Ogden. 1995. Kinetics of cytosolic Ca^{2+} concentration after photolytic release of 1-D-myo-inositol 1,4-bisphosphate 5-phosphorothioate from a caged derivative in guinea pig hepatocytes. *Biophys. J.* 68:2601–2607.